L0 Confirmation with fast, Tsa based tracking in the T-stations

Public Note

Issue:	1
Revision:	0
Reference:	LHCb-118-2007
Created:	July 25, 2007
Last modified:	October 29, 2007

Prepared by: Johannes Albrecht[a], Matthew Needham[b], Herve Terrier[c]

[a]Physikalisches Institut, Uni Heidelberg

[b]EPFL, Lausanne

[c]NIKHEF, Amsterdam

Abstract

A fast tracking algorithm to confirm the high p_T L0 trigger objects with tracks from the T-stations is presented. The L0 trigger candidate is used to define a search window to a potential track. Using this, a seeded track search is performed. The track finding algorithm is based on the *TsaSeeding* algorithm [1]. The efficiency to confirm a true L0 trigger signal is around 96%, the momentum can be measured up to $\Delta p/p$=3%.

Contents

1 Introduction

The trigger is one of the key components of the LHCb experiment. It reduces the rate from 40MHz bunch crossing to 2kHz which are written to tape. The first level of the Trigger (L0, hardware) relies on high transverse momentum (p_T) μ, e, γ, π^0 and charged hadron candidates, decreasing the rate to 1MHz. At a positive L0 decision, the detector data is read out and transfered to a computing farm. The higher level trigger (HLT) is implemented as software algorithm. That will reduce the rate from 1MHz to 2kHz.

The algorithm presented here is developed to be one of the first algorithms to run in the HLT procedure. The basic strategy is to use the high p_T L0 objects as seeds to create a search window in the T-stations and search for tracks there, see Fig. 1. The track search is done with the *TsaSeeding* algorithm [1] which has been adapted to seeded track search.

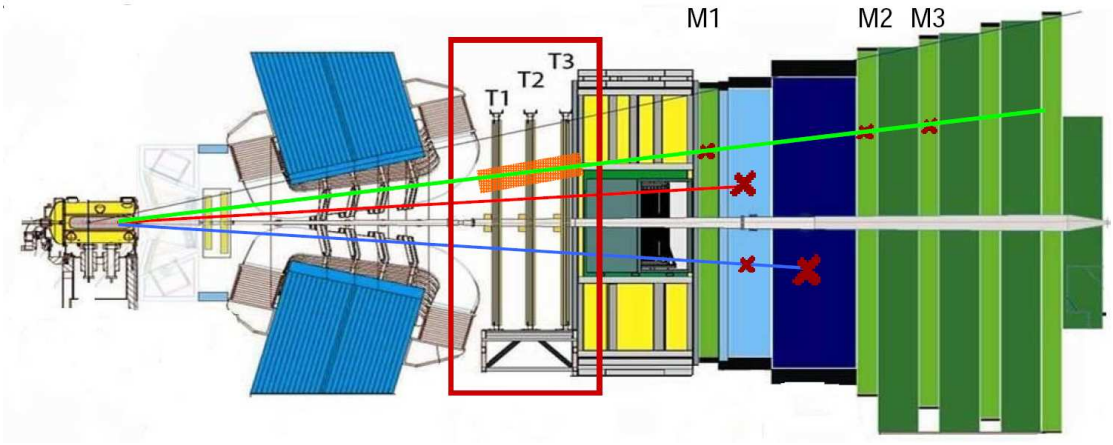

Figure 1 Scheme of the L0 confirmation with T-tracks. Shown is the path of particles traversing the detector for muons (green), electrons (red) and hadrons (blue). The L0 trigger candidate (red crosses) is used as seed to construct a track hypothesis in the T-stations (orange band). From this track hypothesis, the track search is performed.

The algorithm described here is implemented within the full LHCb Gaudi software environment[a]. The simulated data used in this study are part of the DC06 production. The algorithm proceeds as follows:

Seed Preparation: For each L0 candidate a possible track seed is created. In addition to the L0 information, the seed is refined with information from the subdetector where the L0 candidate was measured.

Hit preparation: It is checked which OT modules lie within an area around the track hypothesis of a given seed. Only these modules are decoded and the corresponding hits are prepared.

Pattern recognition: The track finding is done using the *TsaSeed* pattern recognition algorithm on selected hits around the track hypothesis. The track search can further be restricted by the direction information of the track hypothesis.

In this note, the three steps of the L0 confirmation algorithm are described and the performance is discussed.

2 Seed preparation

From the seeding L0 candidate a track hypothesis is obtained using the MuonSeedTool, ElectronSeedTool or HadronSeedTool, respectively. The information given by the L0 candidate is refined using the subdetector information. The track hypothesis is then extrapolated to the tracking stations where

[a] The software versions used are: GAUDI v19r4, LHCB v22r8, Brunel v31r8

it is used to define the region of interest for the track search. The track hypothesis is stored as a LHCb::Track object, track parameters and its uncertainties are stored in the LHCb::State object which is associated to the track object.

In case of muon seeding, position and direction are available from the L0 object. The direction is obtained from the slope of the muon track between the first and second muon station (M1 and M2). From the direction measurement, an estimate of the transverse momentum can be given. In case of calorimeter seeding, only the position and the transverse energy are measured. The direction, however, can be obtained from the correlation between track curvature and deposited energy. Using position, direction and momentum, a track hypothesis of a curved track in the magnetic field can be made.

In the following, the determination of position and direction is described for the three different L0 candidates studied.

2.1 Preparation of seeds from the muon stations

The muon stations are divided in four regions where the granularity is decreasing from the inside to the outside of the detector. Thus, the resolution of the muon track hypothesis is determined separately for the four muon regions.

A L0 muon candidate is created by the trigger hardware using the information of the first three muon stations. As seed position for the track search, the position of the muon candidate as measured in M2 is used. M2 is used since the purity is much higher than at M1 (which is located in front of the calorimeters).

The direction of the seed is then calculated from the difference in the hit position in M1 and M2. In case the muon candidate crosses the border between two regions, two position measurements are saved in M1 for technical reasons. The average of both measurements is then taken as position in M1 [2].

The magnetic field between the muon stations and the third tracking station (T3) is very small, the seed can be extrapolated linearly to T3. From T3 to T1, the field is non-negligible. Therefore, a parabola in the x-direction and a straight line in the y-direction is used in this range. This takes into account the curvature of the particle in the magnetic field. The curvature of the track hypothesis is proportional to the momentum and can thus be estimated from the momentum measurement by the L0 candidate[b].

To study the accuracy of the track hypothesis at the position of the tracking station T3, offline reconstructed tracks matched to the same MC particle as the seed are used. The position of the seed estimate at T3 is compared to the one of the offline reconstructed track. Fig 2 a), b) show the resolution for the innermost (finest) and outermost (coarsest) region of the Muon stations. Not only the position, but the slope t_x in the x-z plane (and t_y in the y-z plane) as well can be used to restrict the track search. Fig. 2 c) and d) show the slope resolution of the track hypothesis at T3 for the same two muon regions. The resolutions for all four regions can be found in the Appendix 8.1. The RMS values of the resolutions in x, y, t_x, t_y are summarized in table 1. A single Gaussian describes the distributions reasonably well, however, to account for tails, the RMS is taken as measure of the resolution. In the following, the standard configuration of 5 times this RMS value is used.

	Region 1	Region 2	Region 3	Region4
x	8mm	15mm	29mm	54mm
y	6mm	10mm	20mm	40mm
t_x	3mrad	4mrad	7mrad	13mrad
t_y	4mrad	6mrad	8mrad	10mrad

Table 1 Resolution of the muon track hypothesis at T3. In incl. J/Ψ events, the four muon regions are equally occupied.

[b] This assumes that the particle originates from (0,0,0).

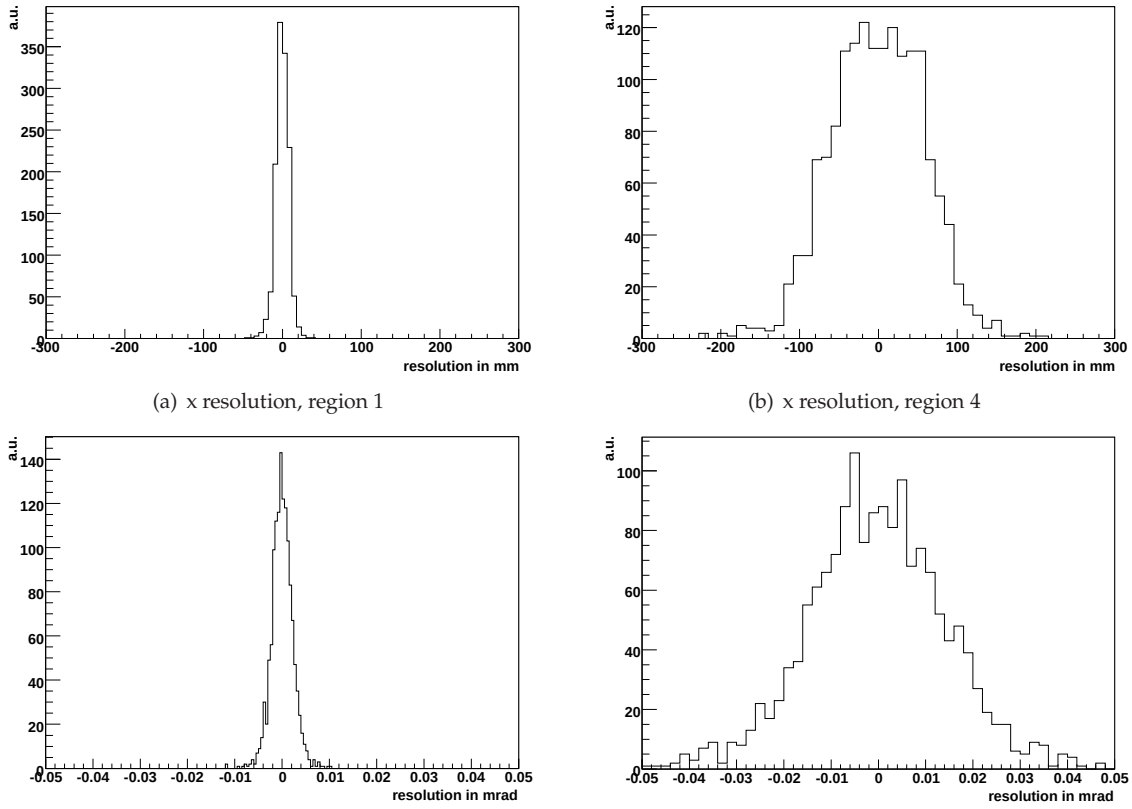

(a) x resolution, region 1

(b) x resolution, region 4

(c) tx resolution, region 1

(d) tx resolution, region 4

Figure 2 Difference between muon track hypothesis at T3 and offline reconstructed track: a), b) show the x-difference for the innermost and the outermost region of the muon stations and c), d) show the slope difference in the same regions.

2.2 Preparation of seeds from the electromagnetic calorimeter

Similar to the muon stations, the electromagnetic calorimeter (ECal) is divided in regions with granularity decreasing to the outside to the detector. The three regions are called: inner part (IP), middle part (MP) and outer part (OP).

The L0 electron candidate consists of a 2x2 cluster in the ECal. In order to refine the position, the 4 cells are decoded. As the decoding of the full ECal takes 1.5ms, the CaloDataProvider tool is used which only decodes the calorimeter banks of interest.

The center of gravity of the 2x2 cluster is calculated. For technical reasons, the cluster position is studied with photons[c]. Fig. 3 a) shows the calculated position in relative coordinates of a cell. An S-shaped deformation from the ideal straight line is clearly visible. This degrades the resolution. However, the shape can be parameterized with a tangent as a function of the relative position inside the cell. It can then be corrected. Fig. 3 b) shows the corrected relative position *vs.* the true position of the cluster. The deformation is removed.

Table 2 summarizes the position resolution of the uncorrected and corrected 2x2 clusters in the ECal. The improvement due to the S-shape correction is clearly visible.

To make a track hypothesis from the ECal cluster, the particle direction has to be determined. The parameterization described here is inspired by the *pt-kick* tool, which is commonly used in LHCb Software (see also section 4.3). As the particle follows a curved track in the magnetic field, the curvature can be approximated from the energy deposit in the calorimeter. The influence of the field is parameterized as a single kick at the center of the magnet. Fig. 4 a) sketches the idea: The difference

[c]On digi files, only the position and direction at the origin of generated particles is saved. For photons, this can be directly extrapolated to the calorimeter using a straight line. Thus, the photon position can be easily used to study the calorimeter measurements.

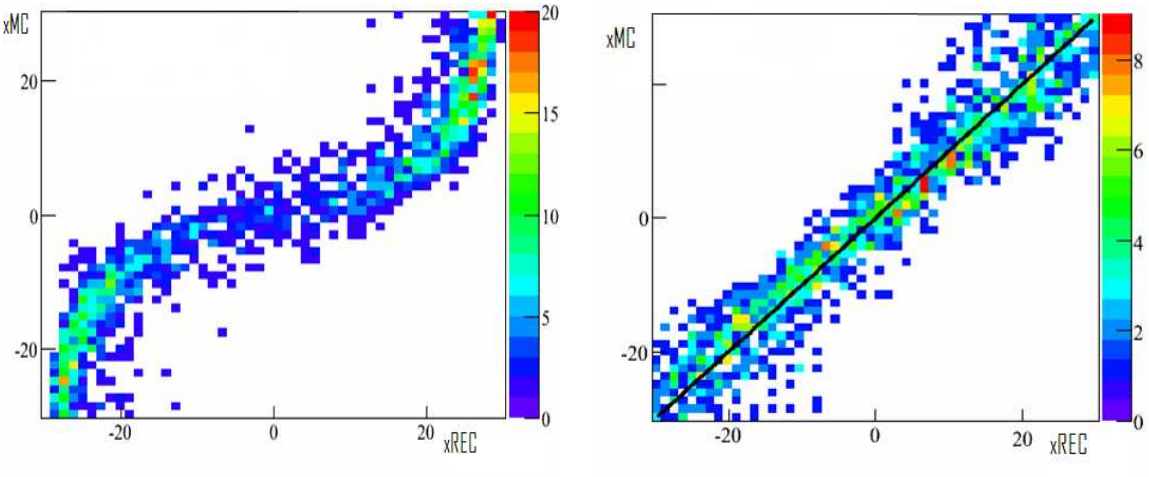

(a) Uncorrected position (b) Corrected position

Figure 3 True position *vs.* reconstructed position in relative coordinates of a cell in the middle part of the ECal. a) Barycenter calculated from the 2x2 cluster. b) Position after the correction for the S-shape.

		ECal IP	ECal MP	ECal OP
uncorrected	x	5.4mm	8.8mm	21mm
	y	5.5mm	9.4mm	21.5mm
corrected	x	2.8mm	5.0mm	12.9mm
	y	3.0mm	5.0mm	12.6mm

Table 2 Resolution of the electron track hypothesis at the ECal.Uncorrected denotes the barycenter of the 2x2 cluster, corrected shows the improved resolution after the S-shape correction.

between the curved particle path (green) and the straight line to the origin (black, dotted) is called Δ. The value of Δ is found to be proportional to the inverse of the cluster energy. The track hypothesis can now be approximated by two straight lines (blue) from the cluster to the focal plane. Of course, two track hypotheses have to be made for the two charge assumptions. Fig. 4 b) shows a parameterization of Δ *vs.* the energy for electrons in minimum bias events. The fitted curve is proportional to $1/E$. From this fit, a direction can be assigned to the ECal cluster yielding to an estimate of the position and slope at the tracking stations. As the charge of the particle is unknown, two search windows for both charge assumptions have to be opened. The parameterization of the particle trajectory between T3 and T1 is as described in the last section.

The resolution of the track hypothesis at T3 (measured with offline reconstructed tracks matched to the same MC particle) is shown in App. 8.2. Table 3 summarizes the the RMS of the resolutions in x, y, t_x and t_y at T3.

2.3 Preparation of seeds from the hadronic calorimeter

The hadronic calorimeter (HCal) is divided in two regions, inner part (HCal IP) and outer part (HCal OP).

	ECal IP	ECal MP	ECal OP
x	3.5mm	5.5mm	15mm
y	5mm	7mm	12mm
t_x	3mrad	3mrad	8mrad
t_y	5mrad	7mrad	8mrad

Table 3 Resolution of the electron track hypothesis at T3. In incl. J/Ψ events, the three ECal regions are equally occupied.

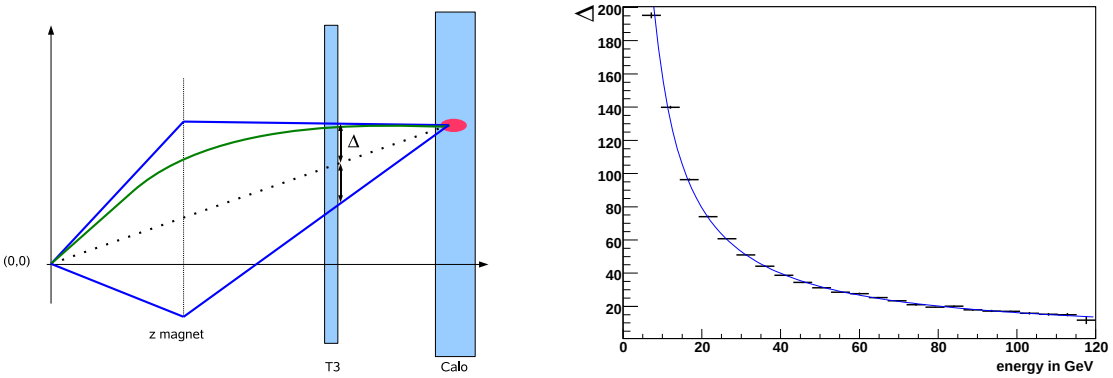

(a) scheme of slope determination (b) Δ *vs.* energy

Figure 4 a) Method to determine the direction for a cluster (see text for a explanation) and b) the parameterization of Δ as a function of the cluster energy. A $1/E$ function has been fitted to the data.

The barycenter of the 2x2 HCal cluster is calculated in a similar way as for the ECal seed. A S-shaped bias in the cluster position is observed. However, the granularity of the HCal is so coarse that it is difficult to correct. This correction is not done here.

In order to utilize the better resolution of the ECal in front of the HCal, the beginning of the hadronic shower in the ECal is used. Therefore, the barycenter is extrapolated to the ECal[d] where 3x3 cells around the extrapolated cluster position are decoded. In these 9 cells, a search for an energy deposit is initiated. The cell center is required to be no further than one cell size (in both x and y) from the extrapolated shower position, giving a maximum of four active cells (see Fig. 5). If more than 2 of these carry energy, the cluster position is determined from the ECal.

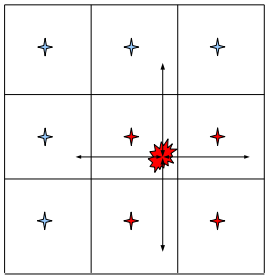

Figure 5 Sketch of the 3x3 ECal cells in front of the HCal. The red star is the cluster position extrapolated from the HCal. The four arrows show the distance of 1 cell size from the extrapolation. All 9 ECal cells shown are decoded. For the position measurement, only the four lower right cells are used since their center lies within ± 1 cell size of the extrapolation.

The slope is approximated from the cluster position in a way similar to the ECal seed. Two different parameterizations are used: for HCal seeding only, and for the case that the ECal can be used as well. The offset Δ is parameterized as a function of the HCal energy only for the first case and as a function of both HCal and ECal energy for the latter. The resolution for the five regions is summarized in table 4. The resolutions of the track hypothesis for x and t_x are shown in Appendix 8.3.

3 Hit preparation

The decoding of the hits in the T-stations is crucial in terms of timing. About 3000 hits in the inner (IT) and outer (OT) tracker are present in an average signal event, see Fig. 6 a). The decoding of the IT is very fast - it takes about 0.1ms to decode the IT hits for the whole event. For the OT, hit

[d] Using a straight line to the origin - this approximation can be made due to the proximity of the two calorimeters.

	HCal + ECal IP	HCal + ECal MP	HCal + ECal OP	HCal IP	HCal OP
x	30mm	31mm	61mm	31mm	100mm
y	26mm	29mm	44mm	26mm	51mm
t_x	17mrad	13mrad	16mrad	15mrad	21mrad
t_y	10mrad	8mrad	18mrad	11mrad	34mrad
fraction	28%	8%	19%	39%	5%

Table 4 Resolution of the hadron track hypothesis at T3. The first three columns describe the case when the ECal in front of the HCal is usable for position determination. The last row gives the fraction of events in each region for incl. J/Ψ events.

decoding via the OTTimeCreator algorithm takes about 2.5ms. This is clearly too slow for trigger applications. Thus, only OT modules where hits are expected are decoded, whereas the whole IT is decoded. Improvements of the decoding algorithms are discussed in section 5.5.

3.1 Decode OT modules on demand

The track hypothesis is used to check which modules lie within the region of the track hypothesis from the L0 candidate. The smallest unit to decode is a read out box of a half module. Generally, this represents 128 channels. In total, the OT consists of 432 such read out boxes.

Around the track hypothesis, a search window is opened of n times the RMS of the track hypothesis (see Tabs. 1, 3 and 4), plus a safety margin of 5cm[e]. It is then checked if the center of the module lies within the search window. To avoid time intensive use of the geometry database, the module geometry is cached into an array structure.

The number of decoded modules is 80 / 40 / 100 for a muon, electron and hadron track hypothesis, respectively. Hence, the number of decoded modules is reduced by a factor of 5-8 with respect to the total detector. Unfortunately, the number of hits to decode does not decrease by the same factor since the majority of hits occurs at small angles with respect to the beam pipe, i.e. in a few central modules. Decoding the OT on demand, the total number of hits to process is reduced from ≈3000 to 800 / 500 / 1000 for a muon, ECal and HCal track hypothesis respectively. Only for these hits, the OTTimes and the TsaClusters are created[f].

3.2 Selection of hits in search window

The crucial point for fast L0 confirmation tracking is to limit as much as possible the number of hits used by the pattern recognition. To select only those hits which lie within the search window, the TsaCollector tool is used. It proceeds as follows:

- Depending on the region (granularity) of the subdetector where the L0 candidate is found, the resolution of the track hypothesis defines the region of interest. The RMS value of these resolutions is given in Tabs. 1, 3 and 4. These RMS values are taken n times, where n depends on the available time budged. In this study, n = 5.
- Before the calculation of the distance between track hypothesis and hit, it is checked if the maximal and the minimal x-value of the wire lies within the search window evaluated at the central z position of the wire (To account for the x-range covered by stereo hits). For x, a safety margin of 0.5cm is applied to include uncertainties due to the bending of the track.
- The distance of closest approach (doca) between the signal wire and the track hypothesis is calculated. This doca is required to be smaller than the search window size of n·RMS(x).

[e] On this level, only the x position at the center of the module is cached. Thus, on stereo modules, the x position depends on y. This effect is absorbed in the 5cm safety margin. Later, on hit level, this is not necessary any more.
[f] This is clearly not optimal as way too many hits are created, see section 5.5 for discussion.

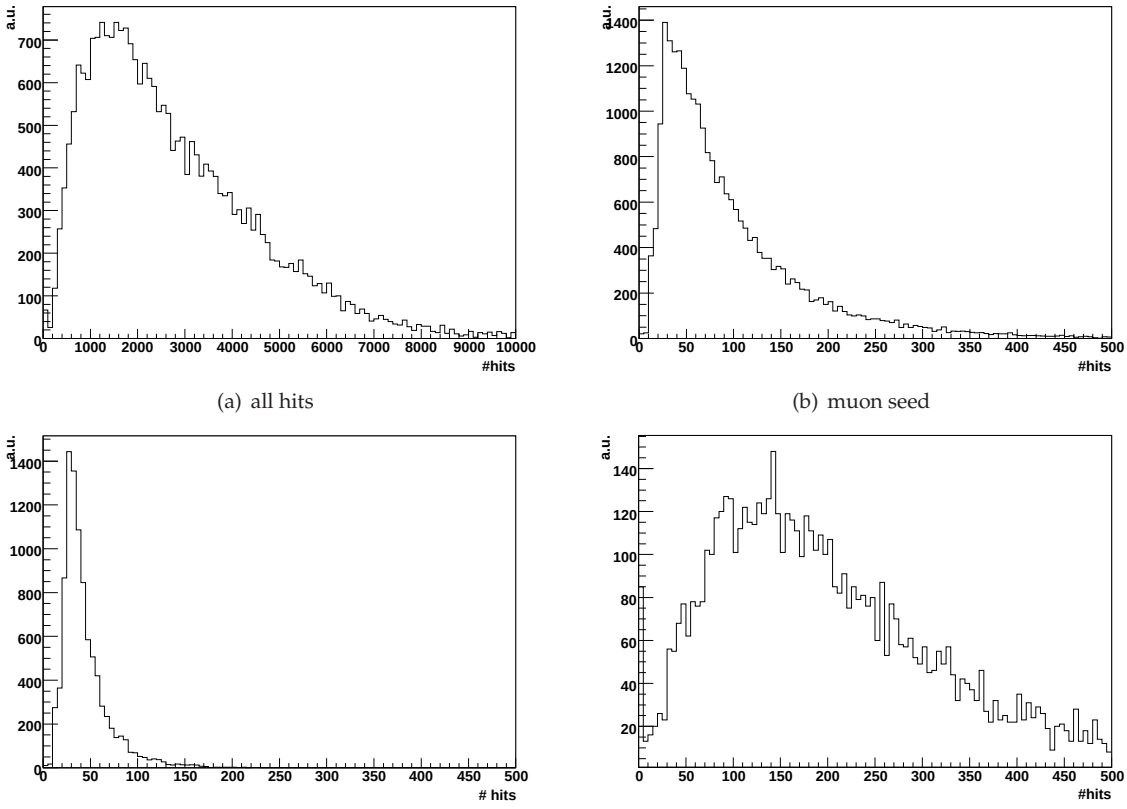

(a) all hits (b) muon seed

(c) ECal seed (d) HCal seed

Figure 6 Number of hits in inclusive J/Ψ events. a) total number of hits in the T-stations (mean: 3000), b) selected hits for muon seeding (99), c) for ECal seeding (43) and d) for HCal seeding (190). Note the different scale of a) compared to b)-d).

- For the OT, the drift radius is calculated using the y-position from the seed. It is required to be within -0.3cm $<$ r$_{drift}$ $<$ 2.8cm.

Fig. 6 a) shows the total number of hits in incl. J/Ψ events. The number of hits accepted in the search window, integrated over all regions is shown in b) for muon, c) ECal and d) HCal seeds respectively. The average number of accepted hits is 99 for muons, 43 for electrons and 190 for hadrons. The difference in the number of hits originates from the different granularities of the two calorimeters and the muon chambers.

4 Track finding

The pattern recognition used for the L0 confirmation is the standard offline seeding algorithm for the T-stations, the *TsaSeeding* algorithm. It is described in detail in Ref. [1]. The main difference, which enables the online algorithm to be run at a rate of 1MHz is the drastic reduction of the number of hits. The tracking is performed on the selected hits for each seed separately. The modifications of the standard *TsaSeeding* algorithm are discussed in the following sections.

4.1 Slope Restriction

The direction of the track can be estimated from the track hypothesis. The resolutions of the slope in the x-z plane (t_x) and in the y-z-plane (t_y) are given in Tabs. 1, 3 and 4. They can be used to restrict the track search.

In the x-search of *TsaSeeding* algorithm, pairs of hits in the first and last stations are used to define a straight line in (x,z), which is later replaced by a parabola. Instead of the generic criterion applied in the *TsaSeeding* algorithm to restrict the slope s_x between the two hits to $|s_x|$ <0.8, the slope between the pair is required to agree within n-times the RMS(t_x) of the track hypothesis. This reduces the number of track candidates at the earliest stage.

In the stereo search, similar to the x-search, pairs of hits in the first and last station are combined to define a line candidate. By default, the slope of the line candidate is required not to differ more than 0.1 from the slope of the straight line obtained by connecting the first hit of the cluster with the origin. Additionally, for L0 confirmation pattern recognition, the slope of each hit with respect to the origin is required to agree within n-times the RMS value of t_y with the track hypothesis.

4.2 Likelihood

Without the restrictions from the track direction, the selection of track candidates is best taken with a track likelihood based on a combination of the number of observed and of expected hits and the χ^2 of a first track fit. The calculation of the likelihood, however, is very time consuming.

This is not necessary any more for the restricted pattern recognition since the number of candidates is reduced. It can be replaced by simple sorting according to the reduced χ^2 of the parabola fit without any loss of efficiency.

4.3 Momentum determination

An estimate of the tracks momentum can be determined with the *pt-kick* tool. Here, the effect of the magnetic field is approximated by a single kick at the point of half the magnetic field crossed. The track is described by two straight lines, one from the T-stations to the magnet bending plane and the other from the bending plane to the origin. The kick in the curvature is given by

$$\Delta curv = \left(\frac{t_x}{1+t_x^2+t_y^2}\right)_T - \left(\frac{t_x}{1+t_x^2+t_y^2}\right)_{origin}, \tag{1}$$

where the first term describes the slope at the T-stations and the second term the slope at the origin. In order to calculate the slope at the origin, the center of the traversed magnetic field has to be known. Thus, the *pt-kick* tool integrates over the B-field for each track. The momentum of the track is proportional to the kick in curvature and the B-field [3]:

$$p = q \cdot (Bdl)_x \cdot \sqrt{\left(\frac{1+t_x^2+t_y^2}{1+t_x^2}\right)_T} \cdot \frac{1}{|\Delta curv|}, \tag{2}$$

where the q denotes the charge, $(Bdl)_x$ the x-component of the traversed magnetic field and t_x, t_y the track slopes at the T-stations. An empirical correction is then applied to Eq. 2. The *pt-kick* method is described in more detail in Ref. [3].

The resulting momentum resolution has a core Gaussian width of 2.4% with an RMS of 7%. However, as one has to integrate over the B-field for each track, the momentum determination takes 0.1ms per track. This is a significant part of the L0 confirmation time.

The transversed magnetic field (B_x) as well as the bending plane (z_{focal}) can be parameterized to reduce the time needed for the momentum determination. The distributions of B_x and z_{focal} are shown in Fig. 7 a,b for a sample of muon tracks from minimum bias events with p_T >0.8GeV. The traversed field is taken to be 4.179Tm and the effective center is set to 5172mm.

The momentum resolution is determined from minimum bias events, using an independent sample compared to the one which the parameterization has been derived from. The momentum resolution is only slightly degraded with respect to the full *pt-kick* tool, whereas the time needed for the momentum calculation is reduced by more than a factor of 20. The momentum resolution is further discussed in section 5.2.

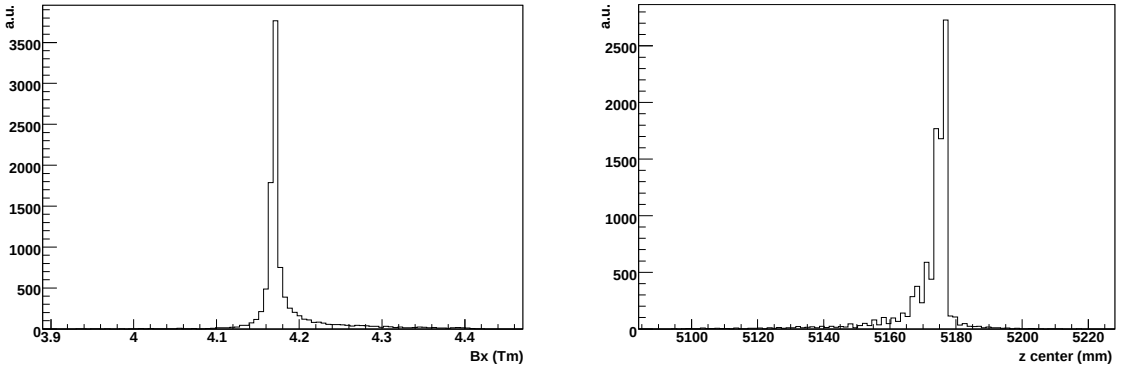

(a) Traversed field B_x (b) Effective center of B_x

Figure 7 Parameters for the fast momentum determination: a) the x-component of the traversed magnetic field (mean: 4.169Tm) and b) the effective center of the field (mean: 5172mm).

5 Performance

There are four important performance measures of the L0 confirmation algorithm: The efficiency to reconstruct a track belonging to the L0 candidate, the number of tracks found per candidate (purity), the momentum resolution and the algorithm execution time.

To determine the performance numbers, the standard configuration of 5·RMS(x), 5·RMS(y), 5·RMS(tx) and 10·RMS(ty) is used. The dependence of the performance on these requirements is discussed in section 5.3. The performance is measured using two track samples:

- A sample of 25000 incl. $J/\Psi -> e^+e^-/\mu^+\mu^-$ events generated at the nominal LHCb luminosity of $2 \cdot 10^{32}\text{cm}^{-2}\text{s}^{-1}$.
- A sample of 25000 minimum bias events generated at the nominal LHCb luminosity of $2 \cdot 10^{32}\text{cm}^{-2}\text{s}^{-1}$.

5.1 Efficiency and number of reconstructed tracks

In order to define an efficiency we need to introduce a denominator (which particles do we want to reconstruct) and a nominator (which particles out of the denominator have actually been reconstructed).

There are two different ways to define the denominator. The first one is based on all MC particles with some additional quality criteria, the second one is based on all particles which have been reconstructed offline. While the first gives an absolute measure of the efficiency, the latter gives the fraction of events which are lost by additional cuts applied in the trigger algorithm which are not present for offline reconstruction.

Efficiency vs. *Monte Carlo*

All particles fulfilling the following criteria enter in the efficiency denominator:

- A reconstructed L0 is associated to it (for muons matching is performed according to the MuonTileId in M2[8]),
- its transverse momentum is larger than 0.8 GeV,
- the MC particle is a μ / e / p,π or K respectively,
- the particle has left at least 1 x and u/v hit per T-station and
- the production vertex of the particle is within 50cm of the origin (0,0,0).

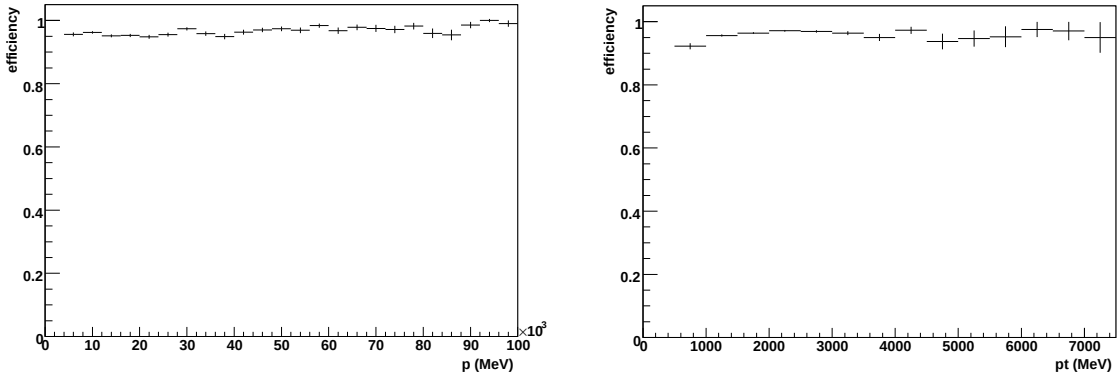

(a) momentum (b) transverse momentum

Figure 8 Efficiency for L0 muon confirmation with respect to MC. The efficiency is flat in both p and p_T throughout the whole momentum range. The inefficiencies of the reconstruction code at low momenta do not occur here since the trigger candidates have a high momentum.

	efficiency *vs.* MC	average #tracks
muon	96.2%	1.3
electron	95.8%	1.02
photon (no track)	-	0.18
hadron	94.4%	6.2

Table 5 Efficiency *vs.* MC and average number of tracks per seed.

A particle is considered as reconstructed if at least one of the tracks[h] found by the L0 confirmation algorithm is associated to it. The efficiency is shown in Fig. 8 for muons as a function of momentum (a) and transverse momentum (b). A summary of the efficiencies for the three seedings is given in table 5. The efficiency is around 96% which is comparable to the offline reconstruction efficiency [4].

Efficiency vs. *offline tracks*

For the trigger, the efficiency relative to the offline reconstruction is important. Thus, additionally to the MC requirements listed above, an offline reconstructed track is required to be matched to the same MC particle. The offline tracks are taken from the STDTightMuon, -Electron or -(Pion+Proton+Kaon) container, respectively. Tab. 6 summarizes the efficiency for all three seeds. The efficiency is about 0.5% higher than without the requirement of the offline match. This means that the online algorithm misses different tracks as the offline algorithm. A reason for the online algorithm to loose tracks is the restriction posed by the search window. In contrary, an advantage of the online algorithm w.r.t. the offline algorithm is the restriction in the candidate selection. Another advantage of the online reconstruction is that no hits are flagged to belong to other tracks and are thus excluded from the track search.

Another point is that in the offline reconstruction, the tracks are reconstructed with the *PatForward* and the *TsaSeeding* algorithm. The best tracks of both algorithms are taken.

If one requires additionally that the offline track is reconstructed with the Tsa algorithm (track history is set to TsaTrack or TrackMatching), the efficiency increases to 98%. The remaining loss of 2% is due to the restrictions given by the track hypothesis.

The reason for the different inefficiencies of the offline and the online tracking remains to be studied further.

[g] The MC matched particle is in 99.98% the same in M3, however, only in 85% the same in M1. This is caused by M1 hits which are due to the high occupancy in M1 wrongly matched.

[h] I.e. has more than 70% of the hits of this MC particle

	efficiency w.r.t. MC & offline	efficiency w.r.t. MC & offline & Tsa
muon	96.7%	98.0%
electron	96.4%	98.1%
hadron	95.3%	98.0%

Table 6 Efficiency *vs.* offline reconstructed tracks and *vs.* tracks being reconstructed offline by the *TsaSeeding* algorithm.

Number of reconstructed tracks

The number of reconstructed tracks gives a measure of the purity of the L0 confirmation. However, it has to be emphasized that a backward match from the online reconstructed tracks to the L0 seed has not been implemented. By this, the number of reconstructed tracks can further be reduced. Table 5 summarizes the number of tracks for incl. J/Ψ events. For muon seeds, on average 1.3 tracks are found per seed.

For ECal seeds, the number of reconstructed tracks gives a handle to differentiate between electrons and photons: Fig. 9 a) shows the number of reconstructed tracks for a ECal seeds associated to electrons. On average, 1.02 tracks are reconstructed in both charge assumptions. Fig. 9 b) shows ECal seeds associated to photons. On average, we reconstruct 0.18 tracks in both search windows.

For hadron seeds, due to the big uncertainty in the search window, on average 6.2 tracks are reconstructed per seed. However, many of these tracks can be removed by a match to the L0 candidate. There, the good position resolution of the track is utilized to check if the track is compatible with the L0 candidate.

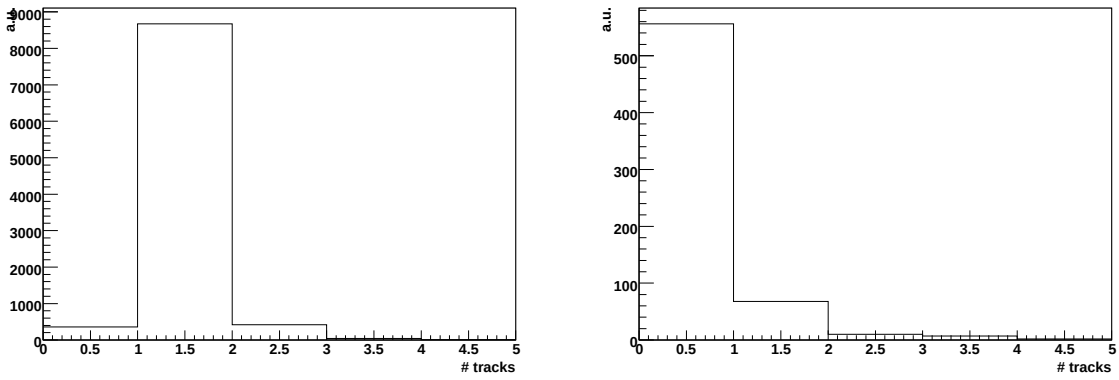

(a) #tracks: true electron (b) #tracks: true photon

Figure 9 Number of tracks found with the L0 confirmation algorithm: a) for ECal seeds associated to electrons and b) for ECal seeds associated to photons.

5.2 Momentum resolution

The momentum of the online reconstructed particles is calculated with the *fast pt-kick* tool (see section 4.3). To determine the resolution, it is compared to the momentum of the associated MC particle.

The momentum resolution is measured with the same acceptance criteria for MC particles as described in the last section. The momentum resolution is determined with a different sample of minimum bias events as the one from which the parameterization was obtained.

Fig. 10 shows the momentum resolution of the L0 candidates which seed the track search (a, c and e) and of the track found to confirm the L0 candidate (b, d and f). For muons, the momentum resolution is improved from ≈30% to 3.0% in the core region. The RMS of this non Gaussian distribution is 8%[i].

[i] This has to be compared to 2.4% core with a RMS of 7% for the full *pt-kick* method.

For electrons, the energy / momentum resolution of the L0 candidate is about 20%. This resolution can be improved to 7% (core above -0.2, 16% RMS). The big tail in the distribution towards too low momenta is caused by bremsstrahlung.

For hadrons, as the granularity of the HCal is very coarse, the energy / momentum resolution of the L0 candidate is ≈40%. The L0 confirmation improves this to 3.8% (core, 11% RMS).

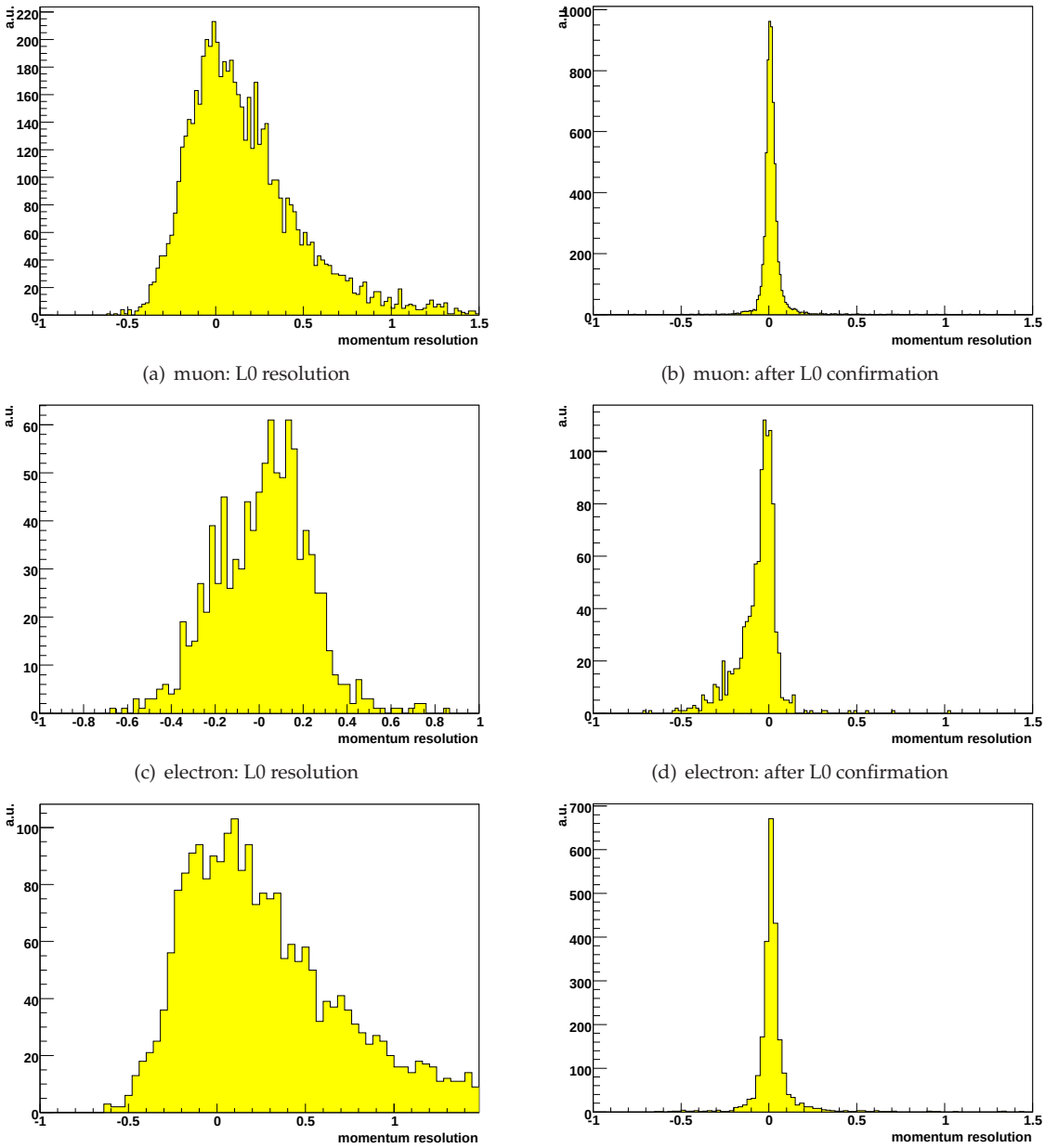

(a) muon: L0 resolution

(b) muon: after L0 confirmation

(c) electron: L0 resolution

(d) electron: after L0 confirmation

(e) hadron: L0 resolution

(f) hadron: after L0 confirmation

Figure 10 Momentum resolution of the L0 candidate (a, c ,e) and of the tracks found by the L0 confirmation algorithm (b, d, f) for muon, electron and hadron seeding respectively.

5.3 Algorithm execution time

algorithm	time muon [ms]	time electron [ms]	time hadron [ms]
L0CandidateFromRaw	0.1	0.1	0.1
Seed preparation	0.02	0.18	0.25
OTTimeCreator*	0.6	0.6	0.8
TsaOTClusterCreator*	0.9	0.6	1.2
CreateITLiteClusters*	0.1	0.1	0.1
TsaSTClusterCreator*	0.5	0.5	0.5
TsaCollector*	1.15	0.7	1.4
L0 confirmation tracking	0.7	0.6	1.5
Sum	4.1	3.4	6.0
Sum w/o decoding	0.8	0.9	1.9

Table 7 Algorithm execution time per event. T-station decoding algorithms are indicated by a star. For electron and hadron confirmation, the tracking time is for both search windows.

The CPU usage of the algorithm has been evaluated on a 2.2GHz-machine (32 bit)[j], using standard LHCb compilation options. A 30% improvement in speed is observed if the machine is run in 64 bit mode. The list of algorithms together with their execution time is given in table 7. The seed preparation time for calorimeter seeds is dominated by the calorimeter decoding on demand. The algorithm execution time spent for hit management decreased from ≈8ms for the decoding of the full OT [5] to ≈3ms. However, the decoding takes with about 80% still the dominant part of L0 confirmation time.

To conclude, the T-station decoding algorithms presented here are clearly not optimal. As described in section 3.1, only relevant modules of the OT are decoded. For these modules, ≈1000 OTTimes and TsaClusters are created of which only ≈100 are selected for track search (by the TsaCollector which loops on the hits). However, since the decoding and hit management will be rewritten in the new track reconstruction framework (see Ref. [6]), it is not further optimized here.

The L0 confirmation tracking algorithm time is taken for one muon seed and for the calorimeter seeded cases for both charge assumptions. The algorithm execution time as a function of the num-

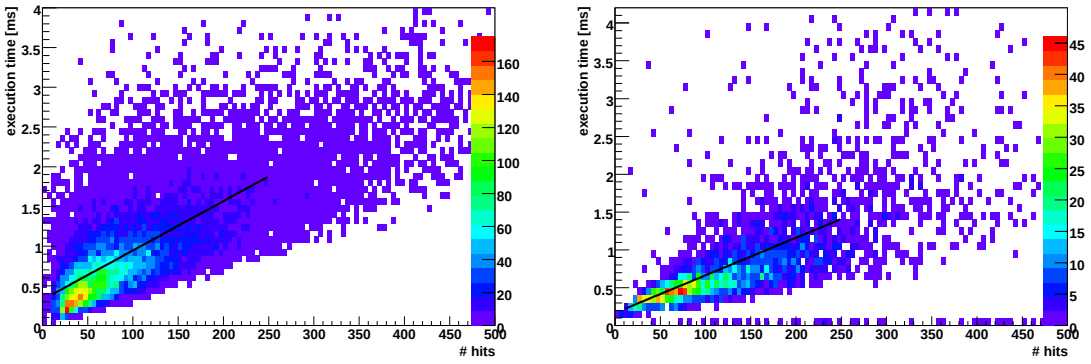

(a) hit collection time (b) track finding time

Figure 11 Algorithm execution time for muon seeds. a) shows the time needed to select the hits in the search window and b) shows the time needed for track search.

ber of selected hits is shown in Fig. 11 for muon seeded L0 confirmation. Fig. 11 a) shows the hit selection time (*TsaCollector*). A straight line is fitted to the profile of Fig. 11 a) in the range of 0 to 250 hits. The observed behavior can be parameterized as a straight line:

$$t = 0.32 + 0.006 \cdot N_{hits}[ms]. \quad (3)$$

[j] According to the standard Brunel output, it is 1.15 times faster than a 2.8 GHz lxplus machine at CERN.

For the hit collection time, a linear behavior at higher hit numbers is expected. The track finding time is shown in Fig. 11 b). It is parameterized as:

$$t = 0.17 + 0.005 \cdot N_{hits}[ms]. \quad (4)$$

The coefficients for electron seeded track search are (0.4,0.004) and for hadron seeded track search (0.22,0.004). Since the number of hits used for track search is very small, only the linear part can be seen here. The quadratic term observed in Ref [1] is not relevant for these low hit numbers.

With the expected improvements in hit handling, the goal of 1ms seems to be well in range for electron, muon and hadron seeded L0 confirmation.

5.4 Efficiency as a function of time

The CPU time needed for track search depends strongly on the size of the region where the track search is performed. However, if we shrink the search window size too much, we loose hits due to the limited accuracy of the track hypothesis. Throughout this study, the standard configuration of 5 times the RMS value of x, t_x and 10 times of t_y was chosen. This configuration gives a nearly maximal efficiency. This point can be seen in Fig. 12 as the third point from the right. Depending on the available CPU time in the HLT, the search window size can be tuned. Especially for hadron seeded track search, compromising on the efficiency can lead to significant time saving.

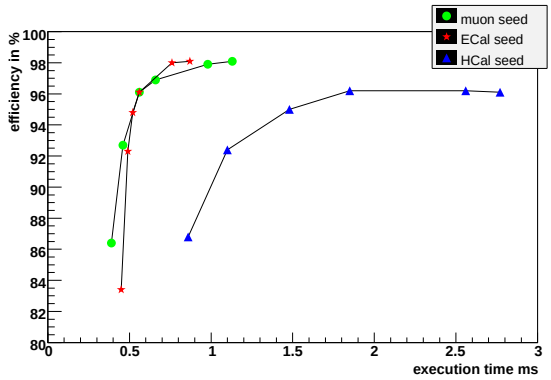

Figure 12 Efficiency *vs.* algorithm execution time for muon (green circle), ECal (red star) and HCal (blue triangle) seeded track search. The different points correspond to variations of the search window. From right to left: ($n \cdot \sigma(x)$,$n \cdot \sigma(t_x)$,$n \cdot \sigma(t_y)$) = (15,15,15), (10,10,10), (5,5,10), (4,4,10), (3,2,10) and (2,2,5). The combination (5,5,10) is used as standard configuration throughout this study.

5.5 Potential improvements

Decoding of the T-stations: The data access tools for track finding are currently being rewritten. There, the decoding of the T-stations will be solved efficiently. The creation of hit classes will be restricted to the region given by the track hypothesis. This will improve the total time needed for T-station decoding by a factor 5-10.

Another possible improvement could be the separate decoding of the x and the stereo layers of the Outer Tracker. After the x-candidate selection, the number of stereo hits to decode can be reduced significantly.

Track search: Already at the level of x-candidate selection, the number of candidates for stereo confirmation can be reduced by a match to the seed.

The source of the different inefficiencies of the online and the offline track search could be further investigated.

Search windows: In the current algorithm, the search window is a constant band around the track hypothesis. The accuracy of the track hypothesis at T3 is about 25% better than at T1. It is as well better for high momentum tracks. Both effects could be included to reduce the search window size.

Momentum determination: In the *fast pt-kick* method, the parameters of the magnetic field could be tuned according to the kinematical region of the track.

6 Conclusion

In this note, an algorithm for fast track finding is presented. The L0 trigger candidate is used to construct a track hypothesis in the T-stations, where a track search is performed. An efficiency of around 96% has been achieved to find a track associated to a L0 muon, electron and hadron candidate. The CPU time needed for tack search depends on the accuracy of the track hypothesis. For muon and electron candidates, it is well below 1ms whereas for hadrons, further improvements are necessary to reach the 1ms goal. Within this time, the momentum measurement can be improved to a core width of $\Delta p/p$=3% for muons, 7% for electrons and 4% for hadrons, respectively.

7 References

[1] R. Forty, M. Needham, *Standalone Track Reconstruction in the T-stations*, LHCb-Note 2007-022

[2] Julien Cogan, *Position of the L0MuonCandidates's pads*, TRec meeting 05-Feb 2007

[3] J. Van Tilburg, *Track simulation and reconstruction in LHCb*, CERN-THESIS-2005-020

[4] R. Forty and M. Needham, *Updated Performance of the T seeding*, LHCb-note 2007-023

[5] J. Albrecht, *L0 confirmation using T-stations*, TRec meeting 02-July 2007

[6] C. Jones, K. Rinnert, S. Hansmann-Menzemer, W. Hulsbergen, *Data handling tools for tracking - interfaces & implementation*, LHCb tracking workshop, 30-August 2007

8 Appendix

8.1 Muon resolution

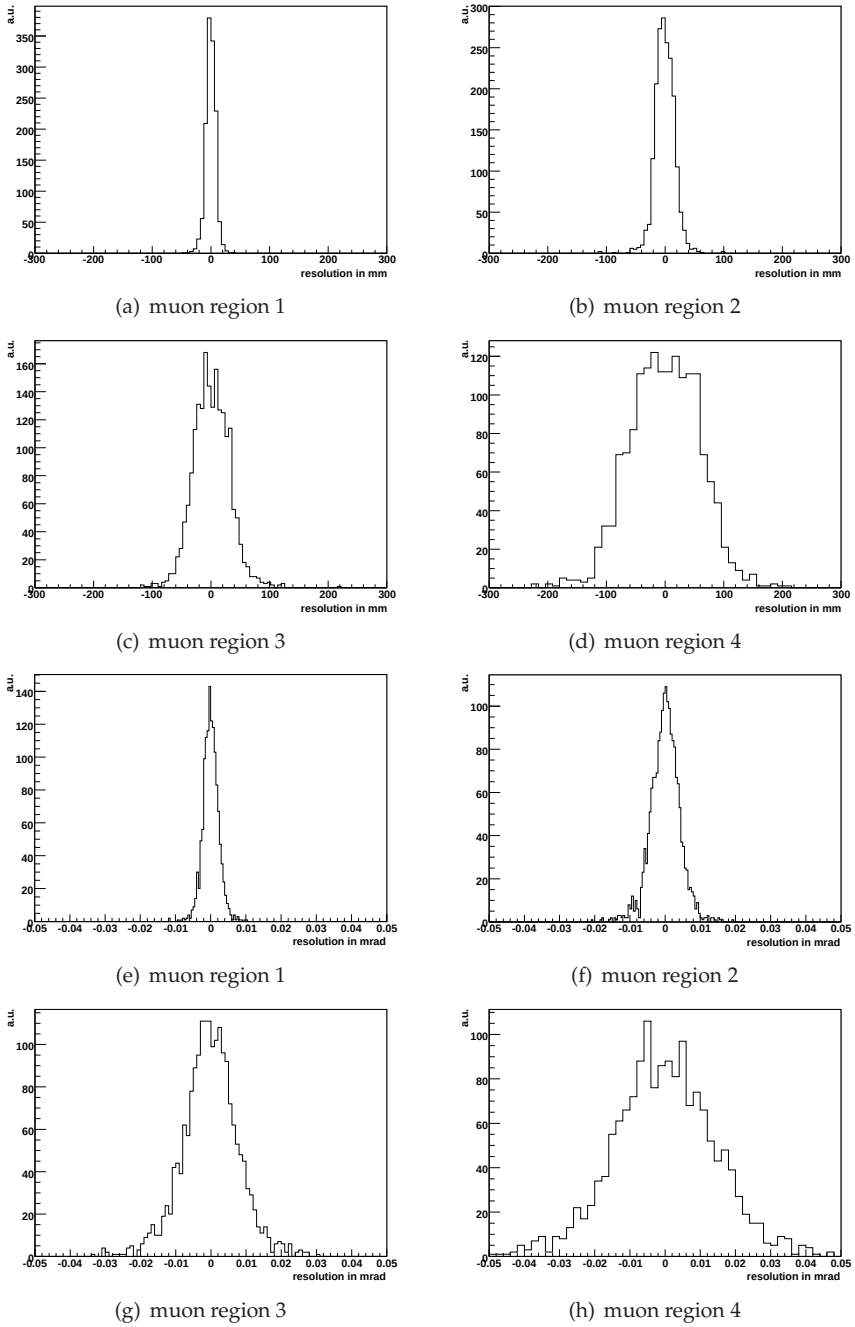

(a) muon region 1 (b) muon region 2

(c) muon region 3 (d) muon region 4

(e) muon region 1 (f) muon region 2

(g) muon region 3 (h) muon region 4

Figure 13 Resolution of the muon track hypothesis for the four regions in x-position (a-d) and in slope (e-h).

8.2 ECal resolution

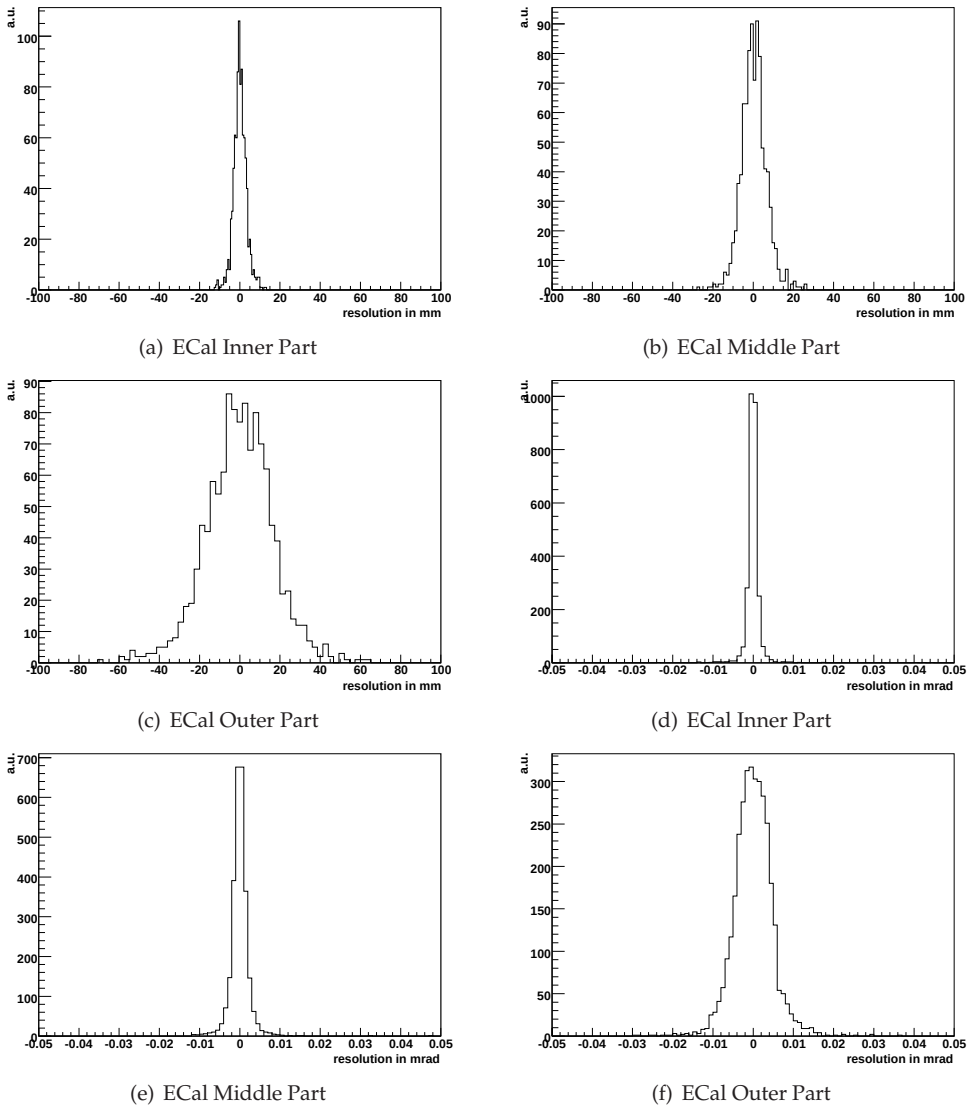

(a) ECal Inner Part (b) ECal Middle Part

(c) ECal Outer Part (d) ECal Inner Part

(e) ECal Middle Part (f) ECal Outer Part

Figure 14 Resolution of the electron track hypothesis for the four regions in x-position (a-d) and in slope in the x-z plane (e-h).

8.3 HCal resolution

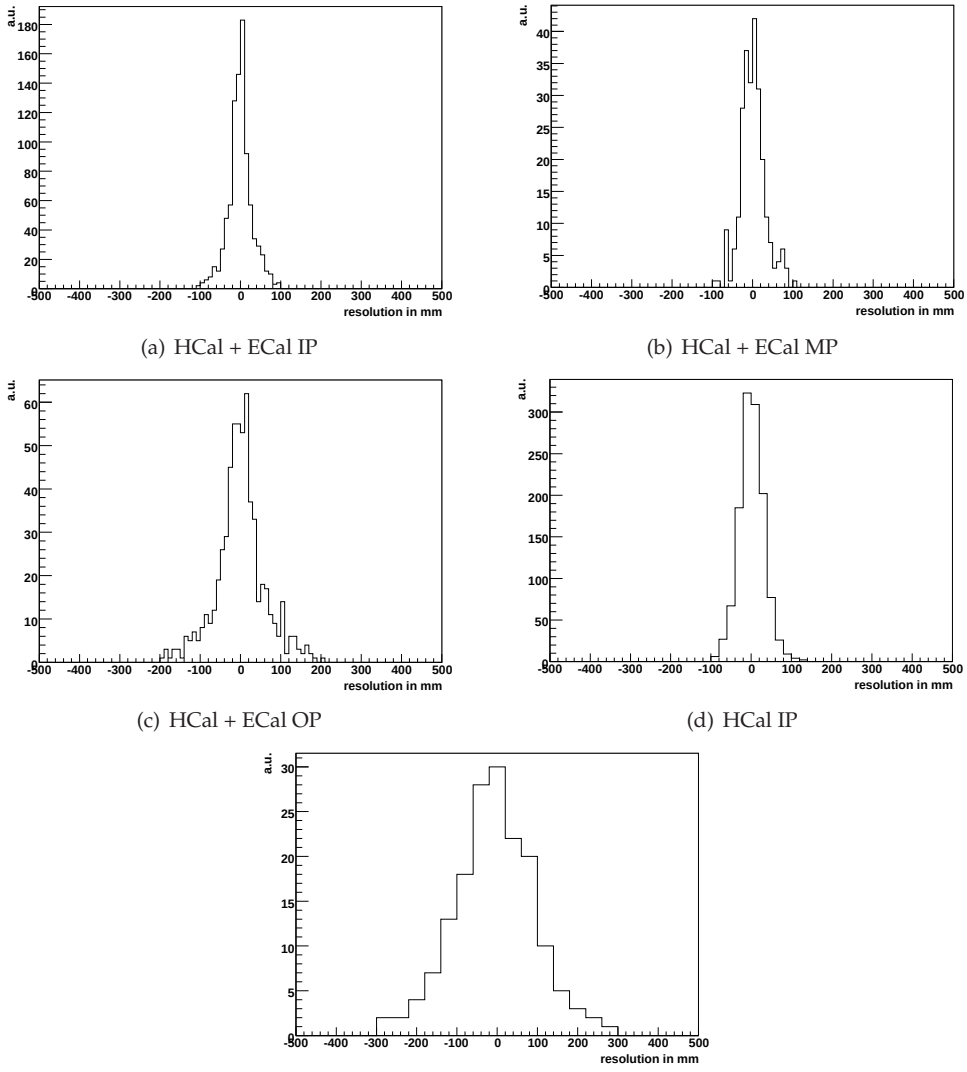

(a) HCal + ECal IP

(b) HCal + ECal MP

(c) HCal + ECal OP

(d) HCal IP

(e) HCal OP

Figure 15 Resolution of the hadron track hypothesis for the five regions in the x-position.

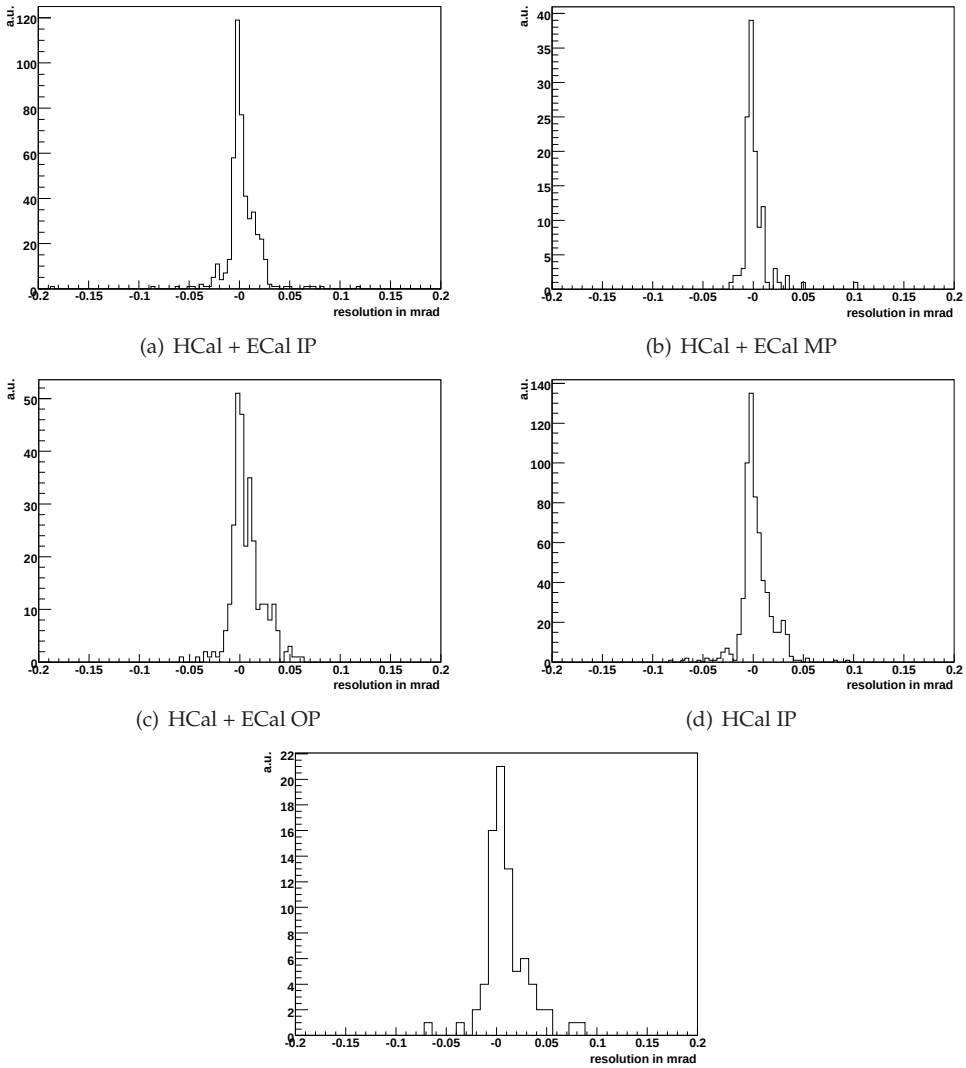

(a) HCal + ECal IP

(b) HCal + ECal MP

(c) HCal + ECal OP

(d) HCal IP

(e) HCal OP

Figure 16 Resolution of the hadron track hypothesis for the five regions in the slope in the x-z-plane.